PHYSICAL REVIEW B **98**, 041109(R) (2018)

Rapid Communications

Thermal plasmon resonantly enhances electron scattering in Dirac/Weyl semimetals

Vladyslav Kozii* and Liang Fu

Department of Physics, Massachusetts Institute of Technology, Cambridge, Massachusetts 02139, USA

(Received 22 April 2018; published 24 July 2018)

We study the inelastic scattering rate due to the Coulomb interaction in three-dimensional Dirac/Weyl semimetals at finite temperature. We show that the perturbation theory diverges because of the long-range nature of the interaction, hence, thermally induced screening must be taken into account. We demonstrate that the scattering rate has a nonmonotonic energy dependence with a sharp peak owing to the resonant decay into thermal plasmons. We also consider the Hubbard interaction for comparison. We show that, in contrast to the Coulomb case, it can be well described by the second-order perturbation theory in a wide energy range.

DOI: 10.1103/PhysRevB.98.041109

Three-dimensional Dirac semimetals have attracted great interest in the condensed matter community due to their exotic electronic properties [1–17]. The low-energy excitations of these materials are massless Dirac fermions with a linear dispersion near the touching points between the conductance and valence bands. If the Kramers degeneracy of the Dirac cones is removed by breaking either time reversal or inversion symmetry, a topological Weyl semimetal (WSM) is realized [3,4]. Weyl nodes are monopoles of Berry curvature in momentum space, hence, they are topological objects and can be eliminated only by merging with another node of opposite monopole strength.

Although noninteracting WSMs are already intriguing due to their nontrivial topological properties, the interaction effects in these materials are of great interest. In particular, inelastic electron-electron scattering is expected to be crucial for determining the conductivity [10,11] and spectral properties [18–20] of clean samples at low temperatures, which can be directly probed in transport and angle-resolved photoemission spectroscopy (ARPES)/scanning tunneling microscopy (STM) measurements, respectively.

While most of the previous studies of the spectral function were focused on the zero-temperature case, certain interesting phenomena are expected in interacting WSMs at finite temperature. For example, finite-lifetime quasiparticles can display novel spectral features described by the non-Hermitian topological theory [21–33]. A call for a profound understanding of these intriguing phenomena that can be measured in ARPES experiments motivates us to study the electron's self-energy in WSMs at finite temperature.

In this Rapid Communication, we focus on the inelastic quantum scattering rate (inverse quasiparticle's lifetime) due to the electron-electron interaction. We consider the cases of the Coulomb and repulsive Hubbard (short-range) interactions. We find that the second-order perturbation theory generically diverges in the case of a Coulomb interaction, and a summation of an infinite series of diagrams within the random phase approximation (RPA) is required. At finite temperature, the collective density oscillations of thermally excited carriers can be considered as thermal plasmons. We show that the thermally induced screening and thermal plasmons lead to a strong energy dependence of the electron scattering rate which exhibits a sharp peak around the plasma frequency $\omega_{\rm pl} \propto T$. This peak can be viewed as a consequence of a strong electron-plasmon interaction. Although we do not aim to describe any specific experiment in our study, we believe it shares similar physics with certain features that were attributed to the coupling between electrons and plasmons and were observed in optical measurements in elemental bismuth [34] and Na_3Bi [35]. Additionally, while we focused on the case of Dirac semimetals in our work, we believe that the same physics is relevant for other semimetallic systems with a low carrier density. For example, we consider half-Heusler compounds with quadratic band touching as promising candidates for testing our findings [36].

Among other results, we find that the scattering rate vanishes logarithmically at exponentially small energies. We also show that the model with the Hubbard interaction, in contrast to the Coulomb case, allows for a perturbative calculation of the scattering rate in a wide range of energies. At the smallest energies, however, it also approaches zero in a nonanalytic way. We hope that our results can be directly probed by measuring the spectral function in ARPES experiments.

Model. We consider a model for WSM at a neutrality point with N identical isotropic Weyl nodes. The low-energy Hamiltonian in the presence of a interaction has the form $H = H_0 + H_{\rm int}$, with

$$H_0 = \sum_{i,\mathbf{k}} \chi_i v_F \psi^\dagger_{\mathbf{k},is} \mathbf{k}\cdot\boldsymbol{\sigma}_{ss'} \psi_{\mathbf{k},is'},$$

$$H_{\rm int} = \frac{1}{2}\sum_{\mathbf{k},\mathbf{p},\mathbf{q}} \psi^\dagger_{\mathbf{k}-\mathbf{q},is}\psi_{\mathbf{k},is} V_0(\mathbf{q}) \psi^\dagger_{\mathbf{p}+\mathbf{q},js'}\psi_{\mathbf{p},js'}. \quad (1)$$

Here, $\psi_{\mathbf{k},is}$ is a two-component spinor in the pseudospin space s, $\boldsymbol{\sigma}$ is a vector of Pauli matrices, $i, j = 1, \ldots, N$ numerate Weyl nodes, $\chi_i = \pm 1$ is the chirality of the ith node, and v_F is the Fermi velocity. A summation over repeating indices is implied. The bare Coulomb interaction is given by $V_0(\mathbf{q}) = 4\pi e^2/\epsilon q^2$, where ϵ is a dielectric constant of a material, and the

*koziiva@mit.edu

repulsive Hubbard interaction is described by $V_0(\mathbf{q}) = \lambda > 0$. In what follows, we neglect the internodal scattering as well as the nonzero curvature of a single-electron spectrum, which, in principle, can play an important role at small energies [37,38], leaving these questions for future study. We use units with $\hbar = k_B = 1$ throughout this Rapid Communication.

The Coulomb interaction. The strength of the Coulomb interaction in Weyl materials is measured by the dimensionless effective fine-structure constant, $\alpha = e^2/\epsilon v_F$, which is a density-independent ratio of a typical Coulomb energy to kinetic energy. Here, we only consider the case of a weak interaction, which is a reasonable assumption for some real materials with a large dielectric constant. For example, fine-structure constants for Bi, Na_3Bi, and Cd_3As_2 can be estimated to be $\alpha_{Bi} \leqslant 0.2$, $\alpha_{Na_3Bi} \approx 0.15$, and $\alpha_{Cd_3As_2} \approx 0.04$ [12,34,35,39–43]. To analytically control our calculation, we further require a large number of Weyl nodes, $N \gg 1$, but keep the product $\alpha N \ll 1$ small. Finally, we also assume that the more restrictive condition is satisfied, $\alpha N \ln(v_F\Lambda/T) \ll 1$, where Λ is a high-momentum cutoff of the order of the distance between nodes. The latter assumption can be easily relaxed and is used here only to simplify some formulas. Despite the approximations made above, we expect our results to be qualitatively correct even for an interaction strength of order one.

Before we consider the inelastic scattering rate, we briefly comment on the velocity and fine-structure renormalization due to the Coulomb interaction. This question was studied, e.g., in Refs. [1,10,44]. It was found that the Fermi velocity and fine-structure constant at the scale of temperature T are renormalized to the leading order as $v_F(T) = v_F(\alpha_0/\alpha_T)^{2/N+2}$ and $\alpha_T = \alpha_0[1 + \frac{(N+2)\alpha_0}{3\pi}\ln(v_F\Lambda/T)]^{-1}$, where v_F and α_0 are bare values at the scale $v_F\Lambda$. We use the renormalized parameters hereafter.

The nonzero scattering rate results from the imaginary part of the interaction potential. Since the bare Coulomb interaction is real, we need to take into account the screening effects, e.g., within the RPA. The effective interaction then has the form

$$V^R(\omega, \mathbf{q}) = \frac{V_0(\mathbf{q})}{1 + V_0(\mathbf{q})N\Pi^R(\omega, \mathbf{q})}, \tag{2}$$

where $\Pi^R(\omega, \mathbf{q})$ is a polarization operator. Generally, the RPA is justified in the limit of a large number of Weyl nodes, $N \gg 1$; however, as discussed in Ref. [45], at finite temperature the RPA is valid even at $N \sim 1$ due to the thermally induced screening, provided relevant momenta satisfy the condition $v_F q \lesssim T$.

While the evaluation of the polarization operator at $T = 0$ is straightforward [46,47], the calculation at finite temperature is a very complicated task that can usually be accomplished only numerically. Nevertheless, following the method used in Ref. [45], we find an approximate analytical expression for Π^R in the most relevant limiting cases [48],

$$\Pi^R(\Omega, Q) = \frac{T^2}{v_F^3}\begin{cases} \frac{1}{6}\left(1 - \frac{|\Omega|}{2Q}\ln\frac{|\Omega|+Q}{|\Omega|-Q}\right) + \frac{Q^2}{3\pi^2}\ln\frac{\tilde{\Lambda}}{\max\{1,|\Omega|\}} + i\frac{Q^2}{6\pi}\tanh\frac{\Omega}{2}, & Q \ll 1,\ Q < |\Omega|, \\ \frac{1}{6}\left(1 - \frac{|\Omega|}{2Q}\ln\frac{Q+|\Omega|}{Q-|\Omega|}\right) + \frac{Q^2}{3\pi^2}\ln\tilde{\Lambda} + i\frac{\pi}{12}\frac{\Omega}{Q}, & Q \ll 1,\ Q > |\Omega|, \\ \frac{Q^2}{3\pi^2}\ln\frac{\tilde{\Lambda}}{\sqrt{\Omega^2-Q^2}} + i\frac{Q^2}{6\pi}\operatorname{sgn}\Omega, & Q \gg 1,\ Q < |\Omega|, \\ \frac{Q^2}{3\pi^2}\ln\frac{\tilde{\Lambda}}{\sqrt{Q^2-\Omega^2}} + i\frac{1}{\pi}e^{-Q}\sinh\Omega, & Q \gg 1,\ Q > |\Omega|, \end{cases} \tag{3}$$

where we defined the dimensionless quantities $Q \equiv v_F q/2T$, $\Omega \equiv \omega/2T$, and $\tilde{\Lambda} \equiv v_F\Lambda/2T$. In the zero-temperature limit, $Q \gg 1$, we reproduce the result by Abrikosov and Beneslavskiĭ [1], $\Pi(\omega, q) = \frac{q^2}{12\pi^2 v_F}\ln\frac{\Lambda}{\sqrt{q^2-\omega^2/v_F^2}}$.

In the static limit, $\omega = 0$, the polarization operator (3) determines the thermally induced screening of the Coulomb potential, and the effective interaction at low momenta takes the form

$$V(\omega = 0, v_F q \ll T) = \frac{4\pi\alpha v_F}{q^2 + l_{\mathrm{scr}}^{-2}}, \tag{4}$$

where the screening length is given by $l_{\mathrm{scr}}^{-1} = \frac{T}{v_F}\sqrt{\frac{2\pi}{3}\alpha N}$.

In the region $v_F q \ll \omega \ll T$, the real part of the polarization operator becomes negative, giving rise to thermally induced plasmon excitations [49,50]. At low momenta, the plasmon dispersion is determined by the equation $1 + NV_0(q)\Pi(\omega \gg v_F q) = 0$, yielding the solution

$$\omega = \omega_{\mathrm{pl}} + \frac{3}{10}\frac{v_F^2 q^2}{\omega_{\mathrm{pl}}} - i\Gamma,$$

$$\omega_{\mathrm{pl}} = T\sqrt{\frac{2\pi}{9}\alpha N} \ll T, \quad \Gamma = \frac{3}{32\pi}\frac{\omega_{\mathrm{pl}}^4}{T^3} \ll \omega_{\mathrm{pl}}. \tag{5}$$

At the neutrality point, the only energy scale is set by temperature, hence, it is natural that $\omega_{\mathrm{pl}} \propto T$. We stress that, at weak coupling, the damping of thermal plasmons in WSMs is small compared to their energy, consequently, they are well-defined collective excitations.

To study the inelastic scattering rate, we calculate the imaginary part of the electron's self-energy $\mathrm{Im}\,\Sigma(\omega, \mathbf{k})$ at finite temperature. As discussed in Ref. [45] in the context of graphene, the electron's self-energy is generally a matrix in the pseudospin basis and can be parametrized as $\Sigma(\varepsilon, \mathbf{k}) = \Sigma_\varepsilon I + \Sigma_v \boldsymbol{\sigma}\cdot\hat{\mathbf{k}}$. It is natural to associate the scattering rate with $\mathrm{Im}\,\Sigma_\varepsilon$ taken on the mass shell, in the spirit of the conventional Fermi liquid (FL),

$$\frac{1}{2\tau(\varepsilon)} \equiv -\mathrm{Im}\,\Sigma_\varepsilon^R(\varepsilon, \mathbf{p})|_{p=|\varepsilon|/v_F}. \tag{6}$$

It is clear that $\tau(\varepsilon) = \tau(-\varepsilon)$ at the neutrality point due to particle-hole symmetry, so we focus on positive energies hereafter.

In the one-loop approximation, the imaginary part of the electron's self-energy reads as [51]

$$\mathrm{Im}\,\Sigma^R_\varepsilon(\varepsilon,\mathbf{k}) = \frac{1}{4}\sum_{i=\pm}\int\frac{d^3q}{(2\pi)^3}\mathrm{Im}\,V^R(\omega_i,\mathbf{q}) \times\left(\coth\frac{\omega_i}{2T}+\tanh\frac{\varepsilon-\omega_i}{2T}\right), \tag{7}$$

where we defined $\omega_\pm \equiv \varepsilon \pm v_F|\mathbf{k}-\mathbf{q}|$. After a straightforward but rather cumbersome calculation, we find [48]

$$\frac{1}{\tau(\varepsilon)} = \begin{cases} c_1\frac{T}{N}\left(\ln\frac{T}{\varepsilon}\right)^{-2}, & \varepsilon \ll T\exp\left(-\frac{c_2}{N\alpha}\right), \\ 2\alpha T, & T\exp\left(-\frac{c_2}{N\alpha}\right) \ll \varepsilon \ll T\sqrt{\alpha N}, \\ \frac{3}{4}\alpha T\ln\frac{1}{\alpha N}, & \varepsilon = T\sqrt{\frac{\pi N\alpha}{18}} = \frac{\omega_{\mathrm{pl}}}{2}, \\ 0.55\alpha T, & \varepsilon \gg T\sqrt{\alpha N}, \end{cases} \tag{8}$$

where c_1 and c_2 are numerical coefficients of order 1. The main contribution to the first region comes from the bosonic frequencies and momenta of order of temperature, which are not accurately captured by Eq. (3), hence, coefficient c_1 cannot be calculated within our approach.

The behavior of the scattering rate as a function of energy is shown in Fig. 1(a). We emphasize that even though we consider a weak-coupling limit, result (8) is nonperturbative. Indeed, the naive lowest-order weak-coupling answer (a single polarization bubble in the effective interaction) would be proportional to $\tau^{-1}_{\mathrm{naive}} \propto \alpha^2 N$, which does not hold in any of the energy domains. This is due to the singular form of the Coulomb interaction at low momenta, which eventually leads to the infrared divergence and requires the RPA resummation. This conclusion is similar to the result for a two-dimensional (2D) analog of the problem, graphene, considered in Ref. [45].

At small energies, $\varepsilon \lesssim 2\alpha T$, the quasiparticles are not well defined, since $\tau^{-1}(\varepsilon) > \varepsilon$ in this range. The scattering rate of these states, however, is determined by electrons with higher energies, which ensures the self-consistency of our calculation. This is in analogy with the conventional FL theory at nonzero temperature, where the finite lifetime of quasiparticles at vanishing energy is determined by thermal excitations. There is, however, an interesting difference between WSM and FL at exponentially small energies, $\varepsilon \ll T\exp(-c_2/\alpha N)$. In this regime, the scattering rate in FL saturates to a constant value, $\tau_{\mathrm{FL}}(\varepsilon\to 0) \propto T^2$, while in WSM it logarithmically approaches zero [see Eq. (8)]. The reason for such behavior is rooted in the logarithmical divergence of the real part of the polarization operator (3) at $|\omega| \approx v_F q \sim T$. For exponentially small energies ε, one has $\ln||\Omega| - Q| \sim \ln(\varepsilon/T)$, which eventually determines $\tau^{-1} \propto \ln^{-2}(T/\varepsilon)$ dependence in this regime.

As the energy of the quasiparticles increases, the scattering rate exhibits a nonmonotonic behavior. In particular, it has a sharp, logarithmically enhanced peak at $\varepsilon = \omega_{\mathrm{pl}}/2$ due to the resonant excitation of the thermal plasmons [48]. This distinctive feature is exclusive for 3D and absent in graphene [45]. At zero temperature, the scattering rate is zero because of phase-space restrictions [18]. Since $\tau^{-1} \sim \alpha T$ for most of energies, WSM with the Coulomb interaction can be called a marginal FL.

Next, we calculate the self-energy in two other important limits, $\mathrm{Im}\,\Sigma_\varepsilon(\varepsilon,\mathbf{k}=0)$ and $\mathrm{Im}\,\Sigma_\varepsilon(\varepsilon=0,\mathbf{k})$, and present our results in Table I. We see that in the region $\varepsilon \ll T\sqrt{\alpha N}$ the answer is nonperturbative and coincides (up to a possible numerical prefactor) with the scattering rate, Eq. (8). At higher energies, on the contrary, one can use second-order perturbation theory. We also notice that the plasmon peak is absent in $\mathrm{Im}\,\Sigma_\varepsilon(\varepsilon,\mathbf{k}=0)$, because the plasmon resonance cannot be achieved in this case due to a frequency-momentum mismatch [48].

Formally, the second-order perturbative result for $\mathrm{Im}\,\Sigma_\varepsilon(\varepsilon,\mathbf{k}=0)$ and $\mathrm{Im}\,\Sigma_\varepsilon(\varepsilon=0,\mathbf{k})$ converges (no infrared divergence in momentum integral) for any nonzero $\varepsilon \neq 0$ or $\xi_{\mathbf{k}} = v_F k \neq 0$. However, upon decreasing the energy of

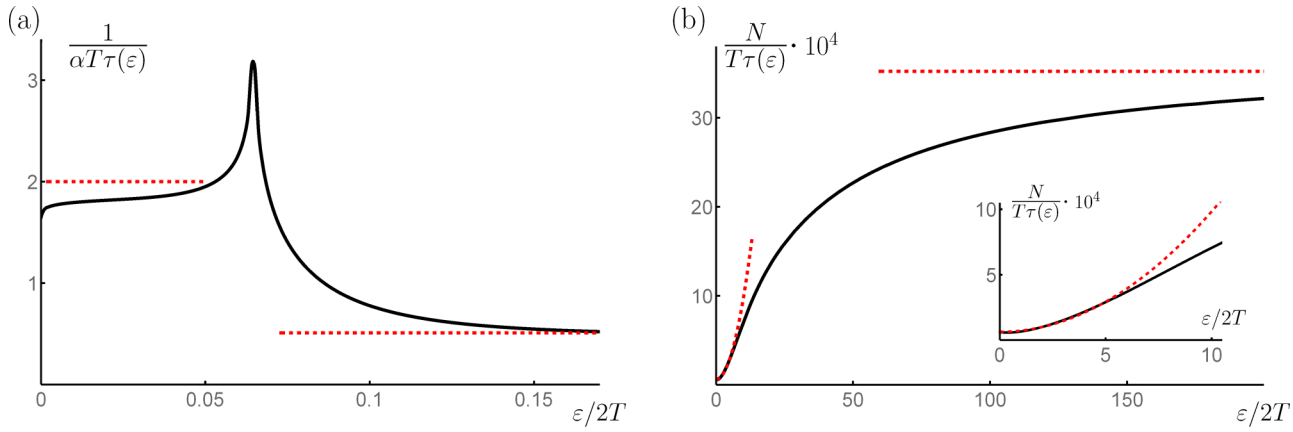

FIG. 1. The inelastic scattering rate as a function of energy due to (a) Coulomb and (b) Hubbard interactions. Red dashed lines correspond to the asymptotic analytical expressions given by Eqs. (8) and (10). At exponentially small energies, the scattering rate logarithmically approaches zero in both cases (not displayed in this figure). (a) The scattering rate exhibits nonmonotonic behavior with a sharp peak at $\varepsilon = \omega_{\mathrm{pl}}/2$ owing to thermal plasmons. The coupling constant equals $\alpha N = 0.1$. (b) Coupling constant λ is such that $\lambda N T^2/v_F^3 = 0.03$. The inset shows that the scattering rate is well described within the second-order perturbation theory (dashed line) in a wide range of energies around $\varepsilon \approx T$. At higher energies, however, the perturbative result smoothly crosses over to a constant, which can only be obtained after the RPA summation. This crossover occurs only for extremely large values of the ultraviolet cutoff Λ satisfying $\Lambda \gg \sqrt{v_F/\lambda N}\ln(v_F\Lambda/T)$.

TABLE I. The imaginary part of the electron's self-energy in the limits of zero energy or momentum due to the Coulomb (top) or the Hubbard (bottom) interactions. The single-electron spectrum is defined as $\xi_{\mathbf{k}} \equiv v_F k$. In the case of the Coulomb interaction, $\mathrm{Im}\,\Sigma_\varepsilon(0,\mathbf{k})$ exhibits a strong peak at $\xi_{\mathbf{k}} = \omega_{\mathrm{pl}}$ due to resonant excitation of the thermal plasmons.

Coulomb	$\varepsilon, \xi_{\mathbf{k}} \ll T e^{-c_2/\alpha N}$	$T e^{-c_2/\alpha N} \ll \varepsilon, \xi_{\mathbf{k}} \ll T\sqrt{\alpha N}$	$\varepsilon, \xi_{\mathbf{k}} = \omega_{\mathrm{pl}}$	$T\sqrt{\alpha N} \ll \varepsilon, \xi_{\mathbf{k}} \ll T$	$\varepsilon, \xi_{\mathbf{k}} \gg T$
$\mathrm{Im}\,\Sigma_\varepsilon(\varepsilon,0)$	$\sim \frac{T}{N\ln^2(T/\varepsilon)}$	αT	$\alpha T/2$	$\frac{2\pi\alpha^2 N T^3}{3\varepsilon^2}$	$\frac{\alpha^2 N\varepsilon}{12\pi}$
$\mathrm{Im}\,\Sigma_\varepsilon(0,\mathbf{k})$	$\sim \frac{T}{N\ln^2(T/\xi_{\mathbf{k}})}$	αT	$\frac{3}{4}\alpha T\ln(1/\alpha N)$	$\frac{2\pi\alpha^2 N T^3}{9\xi_{\mathbf{k}}^2}$	$\frac{2\alpha^2 N T^2\exp(-\xi_{\mathbf{k}}/2T)}{3\pi\xi_{\mathbf{k}}}$
Hubbard	$\varepsilon, \xi_{\mathbf{k}} \ll T\exp\left(-\frac{b_2 v_F^3}{\lambda N T^2}\right)$	$T\exp\left(-\frac{b_2 v_F^3}{\lambda N T^2}\right) \ll \varepsilon, \xi_{\mathbf{k}} \ll T$	$T \ll \varepsilon, \xi_{\mathbf{k}} \ll \sqrt{\frac{v_F^3}{\lambda N\ln(v_F\Lambda/T)}}$		$\varepsilon, \xi_{\mathbf{k}} \gg \sqrt{\frac{v_F^3}{\lambda N\ln(v_F\Lambda/T)}}$
$\mathrm{Im}\,\Sigma_\varepsilon(\varepsilon,0)$	$\sim \frac{T}{N\ln^2(T/\varepsilon)}$	$0.035\frac{\lambda^2 N T^5}{v_F^6}$	$\frac{\lambda^2 N\varepsilon^5}{15360\pi^3 v_F^6}$		$\frac{3\pi\varepsilon}{4N\ln^2(v_F\Lambda/\varepsilon)}$
$\mathrm{Im}\,\Sigma_\varepsilon(0,\mathbf{k})$	$\sim \frac{T}{N\ln^2(T/\xi_{\mathbf{k}})}$	$0.035\frac{\lambda^2 N T^5}{v_F^6}$	$\frac{\lambda^2 N T^2\xi_{\mathbf{k}}^3\exp(-\xi_{\mathbf{k}}/2T)}{384\pi^3 v_F^6}$		$\frac{6\pi T^2\exp(-\xi_{\mathbf{k}}/2T)}{N\xi_{\mathbf{k}}\ln^2(v_F\Lambda/\sqrt{\xi_{\mathbf{k}}T})}$

the excitations, it grows as $1/\varepsilon^2$ due to processes with small momenta transfer, signalizing that the naive perturbation theory becomes insufficient and a full summation of the most divergent terms is required [37,38]. After summation within the RPA, the $1/\varepsilon^2$ behavior crosses over to a physically meaningful nonperturbative result at small energies, $\varepsilon, \xi_{\mathbf{k}} \lesssim T\sqrt{\alpha N}$, as shown in Table I.

The Hubbard interaction. Now we perform a similar analysis for the case of a repulsive Hubbard interaction, which may be relevant for certain cold-atom systems. Since we neglect internodal scattering for simplicity, our model is described by the same Hamiltonian (1) with $V_0(\mathbf{q}) = \lambda$. Again, we assume a weak-coupling limit and large-N approximation to justify the RPA summation where needed. Specifically, we focus on small coupling constants λ satisfying $\lambda N T^2 v_F^{-3} \ll 1$. Furthermore, analogously to the case of the Coulomb interaction, we impose a more restrictive condition, $\lambda N T^2 v_F^{-3}\ln(v_F\Lambda/T) \ll 1$, in order to simplify the final expressions.

Similarly to what we found before, finite temperature generates stable collective excitations. In the case of Hubbard repulsion, those are zero-sound modes, with the dispersion determined by the equation $1 + \lambda N\Pi(\omega,\mathbf{q}) = 0$. In the low-frequency limit $v_F q < \omega \ll T$, we find a solution,

$$\begin{aligned}\omega &= (v_F + \delta v_F)q - i\Gamma(q),\\ \delta v_F &= \frac{2}{e^2}v_F\exp\left(-\frac{12v_F^3}{\lambda N T^2}\right) \ll v_F,\\ \Gamma(q) &= \frac{1}{4\pi e^2}\frac{v_F^4 q^4}{T^3}\exp\left(-\frac{12v_F^3}{\lambda N T^2}\right) \ll \omega. \end{aligned} \tag{9}$$

Since the damping is exponentially small, the zero sound is a well-defined excitation provided its energy is smaller than temperature.

While careful calculation of the scattering rate requires a summation of the infinite RPA series for an effective interaction, it is instructive to first consider the result obtained within the second-order perturbation theory. We find that it gives the answer expected from simple scaling arguments, $\mathrm{Im}\,\Sigma_\varepsilon(\varepsilon,\mathbf{k}) \sim \lambda^2 N v_F^{-6} T^5$ for $\varepsilon, v_F k \ll T$, independently of the ratio $\varepsilon/v_F k$. This is in sharp contrast to the 2D version of the problem studied in Refs. [37,38] or the case of a Coulomb interaction studied above, where perturbation theory completely fails at low energies.

Since the perturbative result does not display any dangerous divergencies, it is tempting to conclude that such an approach is sufficient, and no RPA summation is needed at weak coupling. Though this statement is true in a large energy domain, the correct answer obtained within the RPA is more peculiar,

$$\frac{1}{\tau(\varepsilon)} = \begin{cases} b_1\frac{T}{N}\left(\ln\frac{T}{\varepsilon}\right)^{-2}, & \varepsilon \ll T\exp\left(-\frac{b_2 v_F^3}{\lambda N T^2}\right),\\ 0.07\frac{\lambda^2 N T^5}{v_F^6}, & T\exp\left(-\frac{b_2 v_F^3}{\lambda N T^2}\right) \ll \varepsilon \ll T,\\ \frac{3\zeta(3)+4}{96\pi^3}\lambda^2 N\frac{T^3\varepsilon^2}{v_F^6}, & T \ll \varepsilon \ll \sqrt{\frac{v_F^3}{\lambda N\ln(v_F\Lambda/T)}},\\ \frac{3}{2\pi}\lambda\frac{T^3}{v_F^3}\left(\ln\frac{v_F\Lambda}{T}\right)^{-1}, & \sqrt{\frac{v_F^3}{\lambda N\ln(v_F\Lambda/T)}} \ll \varepsilon \ll v_F\Lambda. \end{cases} \tag{10}$$

Here, $b_{1,2}$ are coefficients of order 1, $\zeta(x)$ is the Riemann zeta function, and we assumed that $\Lambda^2 \gg v_F/\lambda N\ln(v_F\Lambda/T)$ [in the opposite limit, the last interval in Eq. (10) is absent]. We see that, as anticipated, the second-order perturbation theory is applicable in a wide energy range, failing only for exponentially small, $\varepsilon \ll T\exp(-b_2 v_F^3/\lambda N T^2)$, and parametrically large, $\varepsilon \gg \sqrt{v_F^3/\lambda N\ln(v_F\Lambda/T)}$, energies. From a technical perspective, the reason for the deviation from the perturbative result in these regimes is clear: Even though no singularities appear at the second order, a large logarithmical factor shows up in the third order and proliferates with the order of perturbation. Hence, the RPA summation is necessary, resulting in the first and last lines of Eq. (10). The energy dependence of the scattering rate due to the Hubbard interaction is shown in Fig. 1(b).

The results for $\mathrm{Im}\,\Sigma_\varepsilon(\varepsilon,\mathbf{k}=0)$ and $\mathrm{Im}\,\Sigma_\varepsilon(\varepsilon=0,\mathbf{k})$ are summarized in Table I, demonstrating again the relevance of perturbation theory in a big energy interval. Interestingly, the result for the self-energy at zero momentum formally has a simple scaling behavior, $\mathrm{Im}\,\Sigma_\varepsilon(\varepsilon,\mathbf{k}=0) \sim \lambda^2 N\max\{\varepsilon^5, T^5\}$. In practice, however, the prefactor at T^5 is four orders of magnitude larger than that at ε^5, which must be taken into account when applied to real materials. An analogous situation was encountered in the study of the relaxation rate in quantum dots in Ref. [52].

Conclusions. We studied the scattering rate due to a weak electron-electron interaction in three-dimensional Dirac/Weyl semimetals at finite temperature. We considered the cases of Coulomb and Hubbard interactions. We found that in the Hubbard case the scattering rate can be found within the second-order perturbation theory in a wide range of energies. On the

other hand, the Coulomb interaction necessarily requires the RPA summation because of its long-range nature; this results in the nonmonotonic sharply peaked energy dependence of the scattering rate due to thermally induced plasmon resonance. In both cases, the scattering rate nonanalytically approaches zero at exponentially small energies.

Acknowledgments. We are very grateful to Max Metlitski for productive discussions, and to Jonathan Ruhman and Cyprian Lewandowski for reading the manuscript and giving valuable feedback. This work was supported by the DOE Office of Basic Energy Sciences, Division of Materials Sciences and Engineering under Award No. DE-SC0010526.

[1] A. A. Abrikosov and S. D. Beneslavskiĭ, Zh. Eksp. Teor. Fiz. **59**, 1280 (1971) [Sov. Phys. JETP **32**, 699 (1971)].
[2] A. A. Abrikosov, Phys. Rev. B **58**, 2788 (1998).
[3] S. Murakami, New J. Phys. **9**, 356 (2007).
[4] X. Wan, A. M. Turner, A. Vishwanath, and S. Y. Savrasov, Phys. Rev. B **83**, 205101 (2011).
[5] G. Xu, H. Weng, Z. Wang, X. Dai, and Z. Fang, Phys. Rev. Lett. **107**, 186806 (2011).
[6] A. C. Potter, I. Kimchi, and A. Vishwanath, Nat. Commun. **5**, 5161 (2014).
[7] M. Koshino and T. Ando, Phys. Rev. B **81**, 195431 (2010).
[8] K.-Y. Yang, Y.-M. Lu, and Y. Ran, Phys. Rev. B **84**, 075129 (2011).
[9] A. A. Burkov and L. Balents, Phys. Rev. Lett. **107**, 127205 (2011).
[10] P. Hosur, S. A. Parameswaran, and A. Vishwanath, Phys. Rev. Lett. **108**, 046602 (2012).
[11] B. Rosenstein and M. Lewkowicz, Phys. Rev. B **88**, 045108 (2013).
[12] Z. K. Liu, B. Zhou, Y. Zhang, Z. J. Wang, H. M. Weng, D. Prabhakaran, S.-K. Mo, Z. X. Shen, Z. Fang, X. Dai, Z. Hussain, and Y. L. Chen, Science **343**, 864 (2014).
[13] M. Neupane, S.-Y. Xu, R. Sankar, N. Alidoust, G. Bian, C. Liu, I. Belopolski, T.-R. Chang, H.-T. Jeng, H. Lin, A. Bansil, F. Chou, and M. Z. Hasan, Nat. Commun. **5**, 3786 (2014).
[14] S.-Y. Xu, C. Liu, S. K. Kushwaha, R. Sankar, J. W. Krizan, I. Belopolski, M. Neupane, G. Bian, N. Alidoust, T.-R. Chang, H.-T. Jeng, C.-Y. Huang, W.-F. Tsai, H. Lin, P. P. Shibayev, F.-C. Chou, R. J. Cava, and M. Z. Hasan, Science **347**, 294 (2015).
[15] B. Q. Lv, N. Xu, H. M. Weng, J. Z. Ma, P. Richard, X. C. Huang, L. X. Zhao, G. F. Chen, C. E. Matt, F. Bisti, V. N. Strocov, J. Mesot, Z. Fang, X. Dai, T. Qian, M. Shi, and H. Ding, Nat. Phys. **11**, 724 (2015).
[16] N. P. Armitage, E. J. Mele, and A. Vishwanath, Rev. Mod. Phys. **90**, 015001 (2018).
[17] A. Burkov, Annu. Rev. Condens. Matter Phys. **9**, 359 (2018).
[18] J. Hofmann, E. Barnes, and S. Das Sarma, Phys. Rev. B **92**, 045104 (2015).
[19] R. E. Throckmorton, J. Hofmann, E. Barnes, and S. Das Sarma, Phys. Rev. B **92**, 115101 (2015).
[20] F. Setiawan and S. Das Sarma, Phys. Rev. B **92**, 235103 (2015).
[21] V. Kozii and L. Fu, arXiv:1708.05841.
[22] K. Esaki, M. Sato, K. Hasebe, and M. Kohmoto, Phys. Rev. B **84**, 205128 (2011).
[23] S.-D. Liang and G.-Y. Huang, Phys. Rev. A **87**, 012118 (2013).
[24] T. E. Lee, Phys. Rev. Lett. **116**, 133903 (2016).
[25] H. Menke and M. M. Hirschmann, Phys. Rev. B **95**, 174506 (2017).
[26] Y. Xu, S.-T. Wang, and L.-M. Duan, Phys. Rev. Lett. **118**, 045701 (2017).
[27] D. Leykam, K. Y. Bliokh, C. Huang, Y. D. Chong, and F. Nori, Phys. Rev. Lett. **118**, 040401 (2017).
[28] J. González and R. A. Molina, Phys. Rev. B **96**, 045437 (2017).
[29] W. Hu, H. Wang, P. P. Shum, and Y. D. Chong, Phys. Rev. B **95**, 184306 (2017).
[30] H. Shen, B. Zhen, and L. Fu, Phys. Rev. Lett. **120**, 146402 (2018).
[31] A. A. Zyuzin and A. Yu. Zyuzin, Phys. Rev. B **97**, 041203 (2018).
[32] M. Papaj, H. Isobe, and L. Fu, arXiv:1802.00443.
[33] H. Shen and L. Fu, Phys. Rev. Lett. **121**, 026403 (2018).
[34] R. Tediosi, N. P. Armitage, E. Giannini, and D. van der Marel, Phys. Rev. Lett. **99**, 016406 (2007).
[35] G. S. Jenkins, C. Lane, B. Barbiellini, A. B. Sushkov, R. L. Carey, F. Liu, J. W. Krizan, S. K. Kushwaha, Q. Gibson, T.-R. Chang, H.-T. Jeng, H. Lin, R. J. Cava, A. Bansil, and H. D. Drew, Phys. Rev. B **94**, 085121 (2016).
[36] Y. Nakajima, R. Hu, K. Kirshenbaum, A. Hughes, P. Syers, X. Wang, K. Wang, R. Wang, S. R. Saha, D. Pratt, J. W. Lynn, and J. Paglione, Sci. Adv. **1**, e1500242 (2015).
[37] J. Paaske and D. V. Khveshchenko, Physica C **341**, 265 (2000).
[38] A. V. Chubukov and A. M. Tsvelik, Phys. Rev. B **73**, 220503(R) (2006).
[39] Z. Zhu, B. Fauqué, Y. Fuseya, and K. Behnia, Phys. Rev. B **84**, 115137 (2011).
[40] J. Ruhman and P. A. Lee, Phys. Rev. B **96**, 235107 (2017).
[41] T. Liang, Q. Gibson, M. N. Ali, M. Liu, R. J. Cava, and N. P. Ong, Nat. Mater. **14**, 280 (2015).
[42] K. F. Young and H. P. R. Frederikse, J. Phys. Chem. Ref. Data **2**, 313 (1973).
[43] B. Skinner, Phys. Rev. B **90**, 060202(R) (2014).
[44] H. Isobe and N. Nagaosa, Phys. Rev. B **86**, 165127 (2012).
[45] M. Schütt, P. M. Ostrovsky, I. V. Gornyi, and A. D. Mirlin, Phys. Rev. B **83**, 155441 (2011).
[46] M. Lv and S.-C. Zhang, Int. J. Mod. Phys. B **27**, 1350177 (2013).
[47] J. Zhou, H.-R. Chang, and D. Xiao, Phys. Rev. B **91**, 035114 (2015).
[48] See Supplemental Material at http://link.aps.org/supplemental/10.1103/PhysRevB.98.041109 for details on the evaluation of the polarization operator at finite temperature and the calculation of the electron's self-energy.
[49] J. Hofmann and S. Das Sarma, Phys. Rev. B **91**, 241108(R) (2015).
[50] D. E. Kharzeev, R. D. Pisarski, and H.-U. Yee, Phys. Rev. Lett. **115**, 236402 (2015).
[51] A. A. Abrikosov, L. P. Gorkov, and I. E. Dzyaloshinski, *Methods of Quantum Field Theory in Statistical Physics* (Prentice-Hall, Englewood Cliffs, NJ, 1963).
[52] V. A. Kozii and M. A. Skvortsov, Ann. Phys. **371**, 20 (2016).